Blade-coated sol-gel indium-gallium-zinc-oxide for inverted polymer solar cell

Yan-Huei Lee, Pei-Ting Tsai, Chia-Ju Chang, Hsin-Fei Meng, Sheng-Fu Horng, Hsiao-Wen Zan, Hung-Cheng Lin, Hung-Chuan Liu, Mei-Rurng Tseng, and Han-Cheng Yeh

Citation: AIP Advances **6**, 115006 (2016); doi: 10.1063/1.4967288
View online: http://dx.doi.org/10.1063/1.4967288
View Table of Contents: http://aip.scitation.org/toc/adv/6/11
Published by the American Institute of Physics

Blade-coated sol-gel indium-gallium-zinc-oxide for inverted polymer solar cell

Yan-Huei Lee,[1] Pei-Ting Tsai,[2] Chia-Ju Chang,[3] Hsin-Fei Meng,[2,a] Sheng-Fu Horng,[3,a] Hsiao-Wen Zan,[4,a] Hung-Cheng Lin,[4] Hung-Chuan Liu,[4] Mei-Rurng Tseng,[5] and Han-Cheng Yeh[5]

[1]*Institute of Photonics Technologies, National Tsing Hua University, Hsinchu 300, Taiwan*
[2]*Institute of Physics, National Chiao Tung University, Hsinchu 300, Taiwan*
[3]*Institute of Electronic Engineering, National Tsing Hua University, Hsinchu 300, Taiwan*
[4]*Department of Photonics, National Chiao Tung University, Hsinchu 300, Taiwan*
[5]*Material and Chemical Research Laboratories, Industrial Technology Research Institute, Hsinchu 300, Taiwan*

(Received 18 July 2016; accepted 24 October 2016; published online 1 November 2016)

The inverted organic solar cell was fabricated by using sol-gel indium-gallium-zinc-oxide (IGZO) as the electron-transport layer. The IGZO precursor solution was deposited by blade coating with simultaneous substrate heating at 120 °C from the bottom and hot wind from above. Uniform IGZO film of around 30 nm was formed after annealing at 400 °C. Using the blend of low band-gap polymer poly[(4,8-bis-(2-ethylhexyloxy)-benzo(1,2-b:4,5-b')dithiophene)-2,6-diyl-alt- (4-(2-ethylhexanoyl)-thieno [3,4-b]thiophene-)-2-6-diyl)] (PBDTTT-C-T) and [6,6]-Phenyl C_{71} butyric acid methyl ester ([70]PCBM) as the active layer for the inverted organic solar cell, an efficiency of 6.2% was achieved with a blade speed of 180 mm/s for the IGZO. The efficiency of the inverted organic solar cells was found to depend on the coating speed of the IGZO films, which was attributed to the change in the concentration of surface OH groups. Compared to organic solar cells of conventional structure using PBDTTT-C-T: [70]PCBM as active layer, the inverted organic solar cells showed significant improvement in thermal stability. In addition, the chemical composition, as well as the work function of the IGZO film at the surface and inside can be tuned by the blade speed, which may find applications in other areas like thin-film transistors. [http://dx.doi.org/10.1063/1.4967288]

I. INTRODUCTION

Organic solar cell based on conjugated polymer and fullerene derivative is an attractive emerging technology due to its low-cost solution process, flexibility, and the absence of toxic materials in the device. In order to take full advantage of the solution process, a coating method which can be easily scaled up is crucial. The inverted structure of organic solar cell so far appears to be more promising than the conventional structure due to its expected high stability[1] and high efficiency.[2] One of the main reasons for the higher potential stability of the inverted organic solar cell is the absence of the reactive top electrodes with low-work function such as Ca/Al or LiF/Al. Another possible reason is that the conducting polymer poly (3, 4-ethylenedioxythiophene) polystyrene sulfonate (PEDOT:PSS) can be easily replaced by evaporating high-work function top electrode. PEDOT:PSS beneath the active layer in the normal structure is known to reduce the lifetime of organic light-emitting diode[3,4] and is expected to cause stability problems for organic solar cell as well. In the inverted solar cell, zinc oxide (ZnO) is commonly used as the electron-transport layer beneath the organic active layer.

[a]Corresponding authors. meng@mail.nctu.edu.tw; sfhorng@ee.nthu.edu.tw; hsiaowen@mail.nctu.edu.tw

The role is to block the holes and provide a high Fermi level relative to the top electrode to give a high open circuit voltage (V_{oc}). In order to reduce the fabrication cost, solution process based on sol-gel method is preferred to the vacuum deposition such as sputtering. However, most of the reports on the sol-gel process for ZnO in the inverted organic solar cell are based on spin coating, which cannot be scaled up and incompatible with roll-to-roll fabrication. Spray coating is also used for ZnO deposit,[5] but the fabrication on large area is yet to be demonstrated. In order to fulfill the promise of low-cost high-volume fabrication of inverted organic solar cell, both the inorganic electron-transport layer and the organic active layer have to be continuously coated in large area with high uniformity.

In this work we used blade coating to form the electron-transport layer of indium-gallium-zinc-oxide (IGZO) thin film. Blade coating for organic layers in organic light-emitting diode and solar cell has been shown to give high uniformity in large areas.[6,7] In particular, organic solar cell on 20 cm by 30 cm substrate has been demonstrated.[8] Under continuous delivery the coating area is unlimited and the method is compatible with the future roll-to-roll process. Here the application of blade coating is extended from the organic layer to the inorganic layer of oxide semiconductor. IGZO, rather than ZnO, was chosen partially because it has a higher electron mobility which is important to reduce the electric potential loss across the electron transport layer. In fact the field-effect transistors based on IGZO has drawn a great attention due to its high mobility since its discovery.[9–11] Furthermore, IGZO has a higher flexibility to tune the physical properties of the ratios among the elements in the ternary alloy. For example, the Fermi level, surface roughness, and surface energy are critical for the performance of inverted solar cell and could be controlled by the material composition.

We found that uniform IGZO film can be formed by blade coating with the blade speed of up to 250 mm/s. When the organic active layer was also prepared by blade coating, the device performance depends strongly on the IGZO blade speed. Further analysis shows that the chemical composition and the work function of the IGZO film depend on the blade speed. Using low-band-gap polymer poly[(4,8-bis-(2-ethylhexyloxy)-benzo (1,2-b:4,5-b')dithiophene)-2,6-diyl-alt- (4-(2-ethylhexanoyl)-thieno [3,4-b]thiophene-)-2-6-diyl)] (PBDTTT-C-T) as electron donor and [6,6]-Phenyl C_{71} butyric acid methyl ester ([70]PCBM) as acceptor, the highest power conversion efficiency (PCE) was 6.2% with the optimal blade speed of 180 mm/s. For the same organic materials in the bulk heterojunction, such efficiency is similar to the results for spin-coated sol-gel ZnO.[12] Our approach is however much easier to scale up because all the layers are deposited by blade coating except for the evaporated top electrode.

II. EXPERIMENTAL

A. Device fabrication

As shown in FIG. 1, the structure of the inverted organic solar cell is glass/ITO/IGZO/PBDTTT-C-T:[70]PCBM(120 nm)/MoO_3(10 nm)/Al(40 nm). The chemical structure of the low band-gap polymer PBDTTT-C-T and [70]PCBM and the energy band diagram of the are shown in FIG. 2 and FIG. 3. We used PBDTTT-C-T as the donor which was purchased from Solarmer material Inc. and [70]PCBM as the acceptor which was purchased from Solenne (show in FIG. 2). A schematic of our blade coating process is shown in FIG. 4. The blade coating was performed on a hot plate. The blade is cylindrically shaped and the gap between the substrate and the blade was 120 μm. After delivering the solution and activating the blade coater, the wet film was formed. To dry the wet film, hot air was applied to remove the remaining solvent in about 1 to 10 s. The blade speed ranged from 20 to 400 mm/s. The thickness of the dry film could be controlled by adjusting the blade speed. The blade coating was performed using a home-built machine, which was controlled by a motor.

A pre-patterned indium-tin-oxide (ITO) glass was used as the substrate. The ITO glass substrates were first cleaned by ultrasonic agitation with acetone and isopropyl alcohol, rinsed with deionized water and exposed to UV ozone cleaner for 10 min. The IGZO solution was prepared by dissolving Indium Carbonate, Gallium (III) Nitrate Hydrate and Zinc Methacrylate in 2-methoxyethanol

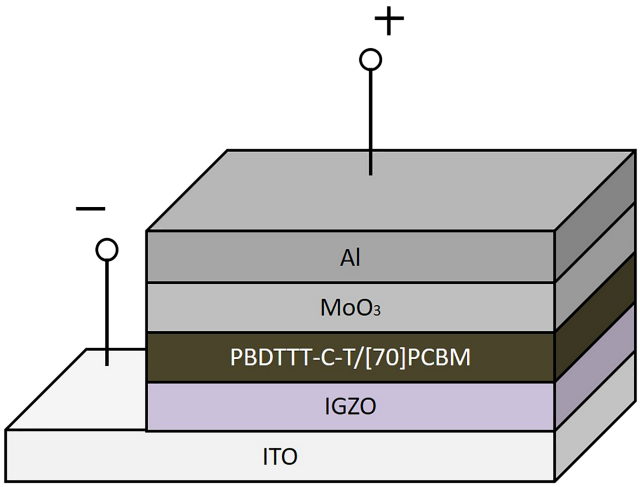

FIG. 1. The structure of device.

with the nominal atomic ratio of In:Ga:Zn=4:1:2 at 0.076 M. After stirring the In-Ga-Zn solution for 24 h, the precursor solution of 30 μl was deposited on the ITO substrates by blade coating to cover the 4 mm^2 active area. The hotplate under the blade coating was about 80 °C. To dry the wet film and enhance the uniformity, the hot wind was applied to the wet film in approximately 6 s. The thickness of the electron transporting layer was 20-30 nm. The IGZO film was then placed in the furnace for annealing at a heating rate of 10 °C/min to a final temperature of 400 °C, and maintained at this temperature for 1 h before cooling in air to room temperature. IGZO had to be patterned to avoid the leakage current between the cathode and the anode of the solar cell. A thermal treatment is necessary for IGZO film in order to enhance mechanical properties and structural stability, densification and grain growth. However, the IGZO layer has high electrical conductivity and was difficult to remove after thermal process. When current leaks out of the intended circuit, instead of flowing through some alternate path, this sort of leakage is undesirable. All residues on the isolation region must be removed. Therefore, a good patterning of IGZO can avoid the leakage current between the cathode and anode of the solar cell. The IGZO film was first covered by patterned photo-resist (AF-5040, Chang Chun Group). The photo-resist was

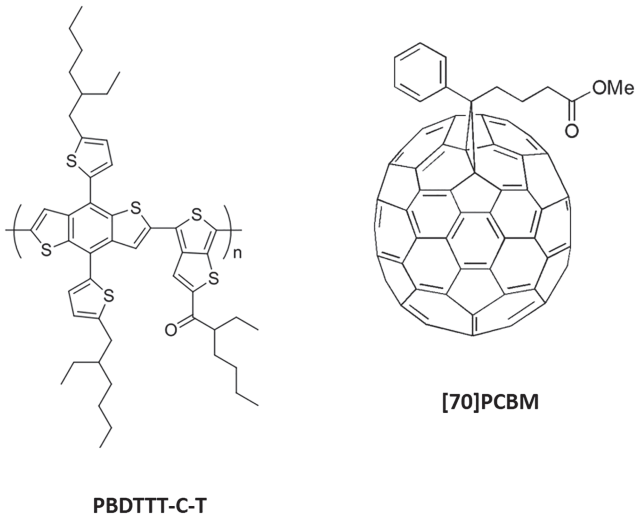

FIG. 2. The chemical structure.

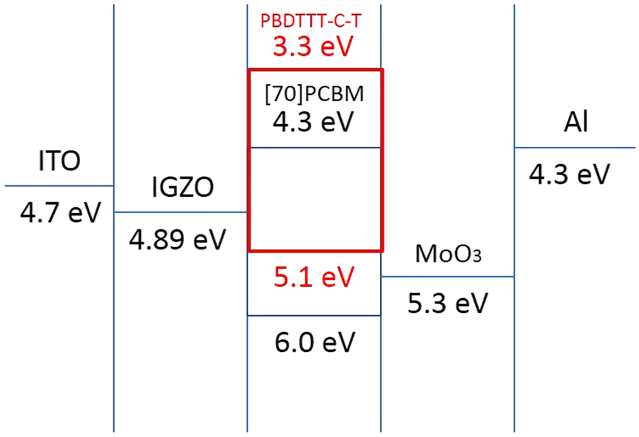

FIG. 3. Energy band diagrams of PBDTTT-C-T/[70]PCBM solar cells which IGZO blade speed was 180 mm/s.

heated at 120 °C for 1 minute to improve the hardness. The sample was then immersed in 12-M HCl for 10 s to etch the exposed part of IGZO. The HCl etching was done after the IGZO furnace annealing.

The powder of the PBDTTT-C-T and [70]PCBM was mixed to prepare the solution of active layer and the weight ratio was 1:1.5, dissolving in toluene. Before coating the active layer, about 3 wt% 1,8-diiodooctane (DIO) was added in the solution as an additive which could improve photovoltaic results.[13–15] The mixed solution was heated at 80 °C then blade coated using 15 μl of solution with the hotplate at 80 °C. After blade coating the organic solution, the hot wind was applied immediately for 6 s to dry the film. The PBDTTT-C-T:[70]PCBM layer was annealed at 120 °C for 20 minutes. The thickness of the dry film was 120 nm. Finally, thermal evaporation in a vacuum chamber with a base pressure under 3.0×10^{-6} torr was used to form the MoO_3(10 nm)/Al(40 nm) as electrode on the top of the active layer, followed by glass encapsulation of the device in a glove box.

B. Device characterization

The J-V characteristics of the solar cell devices were measured using 100 $mWcm^{-2}$ AM 1.5 G solar simulator (XES-301S, SAN-EI). The intensity of incident solar illumination was calibrated by the silicon photodiode (HAMAMATSU S1337-BR). The work function of IGZO was measured by air photo-emission (AC2; Riken Keiki). The X-Ray Photoelectron Spectroscopy (XPS, AES 650, PHI Quantera SXM/Auger) measurements were conducted in an ultra-vacuum system (under 5×10^{-8} torr). The XPS spectra were measured utilizing Al Ka X-ray source for surface and depth profile of the IGZO film. The structure property of the IGZO film was checked by using X-ray diffraction (D1, Bede). Surface roughness and morphology of the IGZO film were observed by atomic force microscopy (AFM, SPA-300HV, SII Nanotechnology Inc). The power conversion efficiency (PCE)

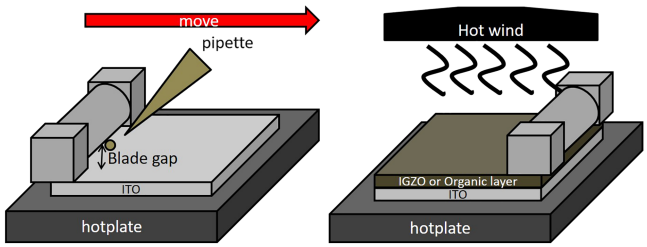

FIG. 4. Schematic illustrating of blade coating method.

was measured using a solar simulator (XES-301S, SAN-EI) under AM1.5G of irradiation To avoid overestimating the aperture loss, PCE was calculated by dividing the photovoltaic power output at AM 1.5G by the total active area. The absorption spectrum was measured using a UV-visible spectrophotometer (cary50, Agilent Technologies).

III. RESULTS AND DISCUSSION

A. Device performance

The blade coating process for the sol-gel precursor of IGZO is shown in FIG. 4. The details were similar to blade coating of organic layers and were reported elsewhere.[16–23] Smooth and uniform IGZO film can be obtained from blade speed below certain values.[24] In FIG. 5 the pictures of a 3 cm by 3 cm film are compared for a low blade speed of 50 mm/s and a high speed of 350 mm/s. For the film coated with high speed, waves and poor uniformity were observed. It was probably due to the solution turbulence, which caused by the shear between the rapidly-moving blade and the substrate. On the other hand, when the blade speed was low, the capillary action at the gap may stabilize the sol-gel solution. The picture of the IGZO film formed by spin coating is also shown for comparison. At a low spin rate of 500 rpm it did give good results, but for high spin rate of 1500 rpm the uniformity was improved. As discussed above the main problem for spin coating is its incompatibility with continuous large-area fabrication. The device performance for the blade speed from 50 mm/s to 250 mm/s is shown in FIG. 6. Uniform IGZO film was uniform in all cases. The active region is 2 mm by 2 mm. The performance for the device of 180 mm/s was significantly better than the devices of 50 mm/s and 250 mm/s. The characteristics are summarized in TABLE I. The mean power conversion efficiency was 5.57% for 180 mm/s. When the speed increased to 250 mm/s the efficiency dropped slightly to 5.05% due to the reduced fill factor. However, when the blade speed was decreased to 50 mm/s, the efficiency dropped sharply to 3.78%, mostly due to the greatly diminished short-circuit current J_{sc}. The EQE spectrum is shown in FIG. 7 for the device of 180 mm/s together with the absorbance of the organic bulk hetero-junction film over IGZO. After integrating the EQE with the AM1.5 solar spectrum, the photo-current is 18.97 mA/cm^2. This is within 10% deviation from J_{sc}.

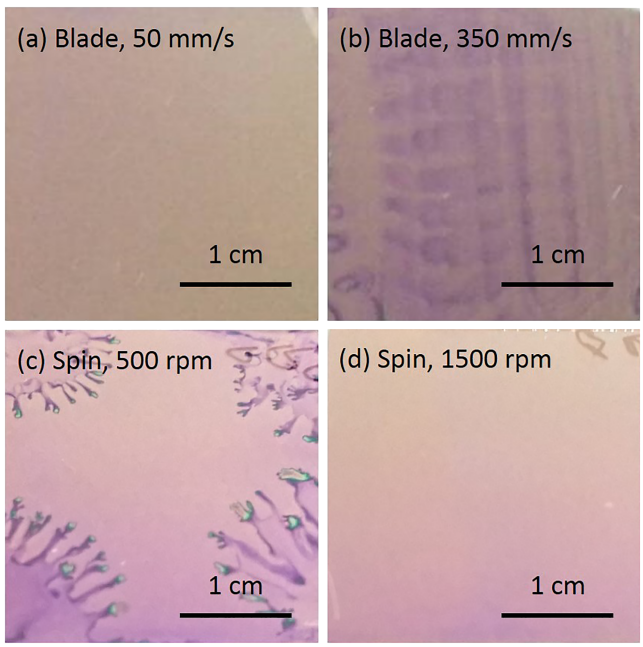

FIG. 5. The IGZO films with (a) low blade speed, (b) high blade speed, (c) low spin speed, and (d) high spin speed.

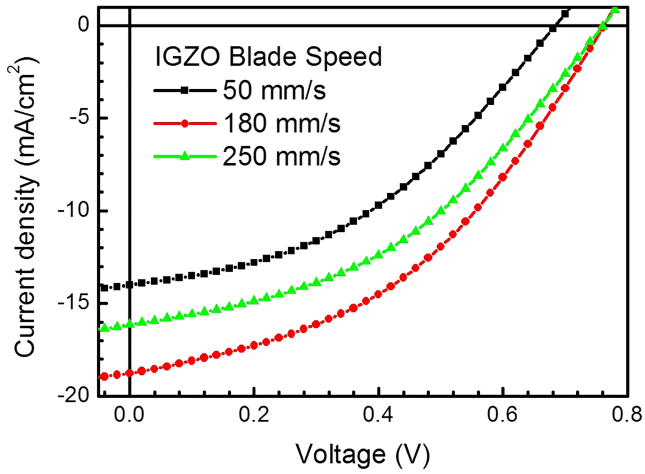

FIG. 6. J-V cure of PBDTTT-C-T/[70]PCBM solar cells which electron transporting layer blade with different speed.

TABLE I. Photovoltaic parameters for PBDTT-C-T/[70]PCBM solar cells and work function of IGZO with different sol-gel IGZO blade speed.

IGZO blade speed (mm/s)	PCE (%)	Jsc (mA/cm^2)	Voc (V)	FF	Work function (eV)
50	3.78 ± 0.08	13.96 ± 0.06	0.68 ± 0.01	0.40 ± 0.00	4.48
180	5.57 ± 0.35	16.88 ± 1.37	0.76 ± 0.00	0.43 ± 0.01	4.89
250	5.05 ± 0.20	16.12 ± 0.28	0.77 ± 0.01	0.41 ± 0.01	4.63

B. IGZO film and blade speed

Various methods were used to characterize the difference among the IGZO film deposited by different blade speed. The scanning electron microscope (SEM) images for the cross section of the devices are shown in FIG. 8. The boundary between ITO and IGZO was not visible, so the IGZO thickness could only be estimated by the total thickness of ITO plus IGZO. The total thickness was 263 nm for blade speed of 50 mm/s, 279 nm for 180 mm/s and 281 nm for 250 mm/s. Since the ITO thickness was about 250 nm, the data could only provide an upper bound of 20-30 nm for IGZO in all cases. The atomic force microscope (AFM) images for various blade speeds are shown in FIG. 9.

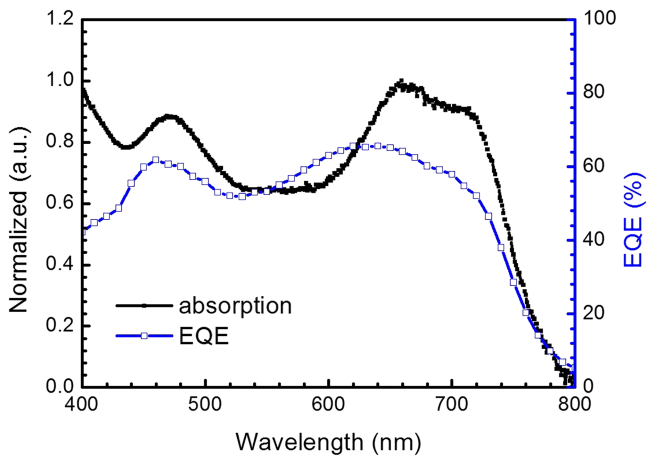

FIG. 7. The absorption spectrum and IPCE spectrum of PBDTTT-C-T/[70]PCBM which blade speed of IGZO was 180mm/s.

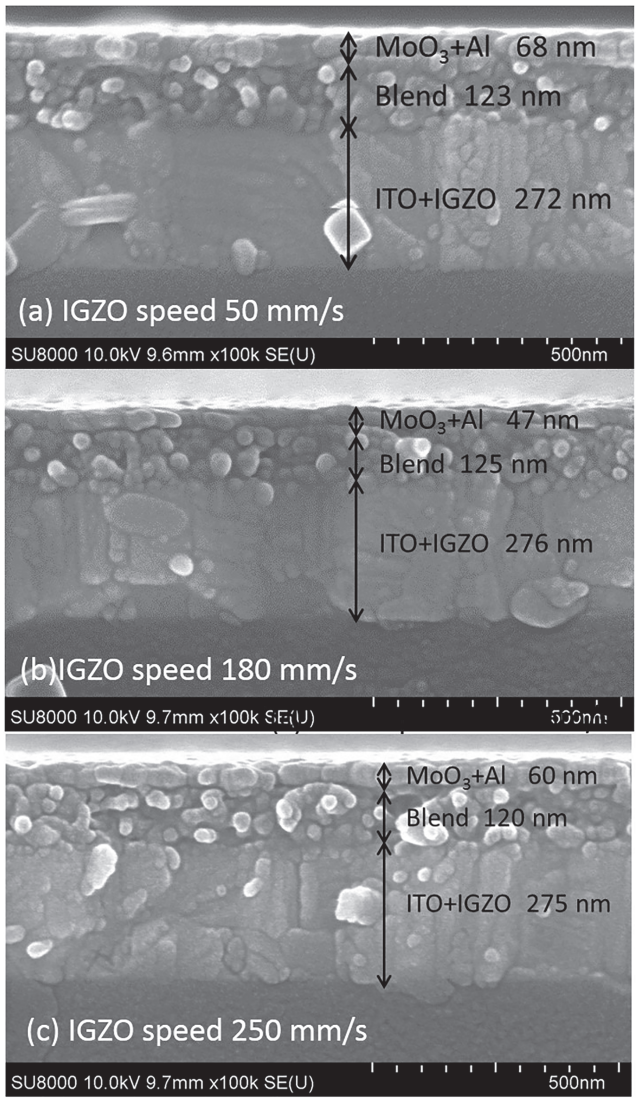

FIG. 8. The SEM images for sol-gel IGZO with different blade speed.

The roughness is about the same for all blade speed. But overall the roughness around 2.5 nm was low enough for the subsequent deposition of the active organic active layer. The crystallinity of the IGZO film was checked by the X-ray diffraction (XRD) and the results are shown in FIG. 10. Only diffraction peaks from ITO were observed, indicating that all the IGZO films were amorphous for all blade speeds in our studies. The depth profile of the atomic composition was determined by the XPS spectrum versus sputtering time in FIG. 11 with argon ion. Interestingly the atomic profile depended

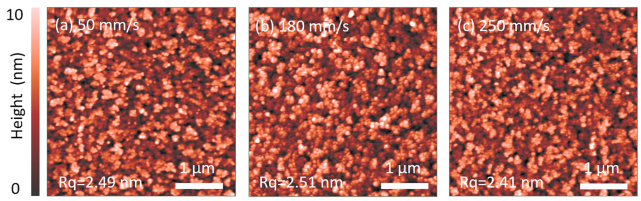

FIG. 9. The AFM topography images for different sol-gel IGZO blade speed (a) 50 mm/s, (b)180 mm/s and (c)250 mm/s.

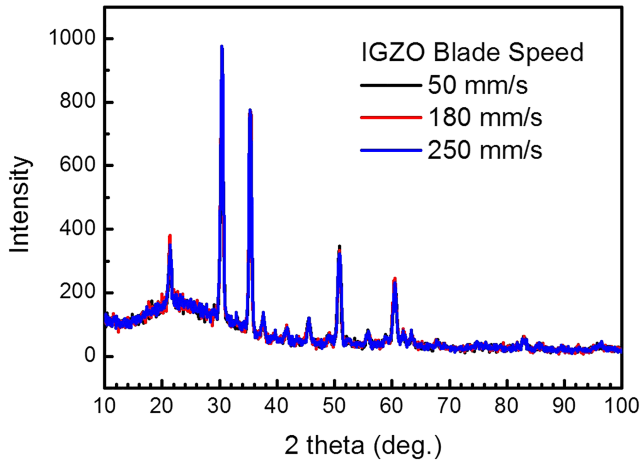

FIG. 10. The XRD diffraction patter of IGZO film in different blade speed.

strongly on the blade speed. In particular, the In concentration was much higher in lower blade speed of 50 mm/s. After a certain sputtering time the Zn signal disappeared because the ion etching reached the ITO layer. The IGZO sputtering time increased with blade speed, and the thickness was roughly estimated by the sputtering rate to be 7.3 nm for 50 mm/s, 17.7 nm for 180 mm/s and 22.1 nm for 250 mm/s. The increase of the thickness with blade speed was consistent with the results for blade coating of organic layers.[6,19,20] The work function was measured by the air photo-emission and the results were 4.48 eV, 4.89 eV, and 4.63 eV for blade speed of 50, 180, and 250 mm/s respectively. The result of 4.4 eV for ZnO was also shown for comparison. The IGZO work function was, however, contrary to the expected trend that lower work function gives higher PCE. The dependence of PCE on the blade speed was therefore not due to the work function and built-in voltage. The work function differences were, however, related to the In concentration at the surface. For low blade speed of 50 mm/s the indium concentration at the surface was the highest as shown in FIG. 11. High indium concentration usually gives high n-doping, corresponding to the Fermi level closer to the vacuum level. Indeed the low blade speed of 50 mm/s gave the lowest work function of 4.48 eV. The surface chemical composition was further checked by the high resolution XPS, and the results are shown in FIG. 12. We focus on the oxygen spectral shape, which was a superposition of oxygen in lattice, oxygen in lattice with oxygen deficiency, as well as oxygen in OH group. After de-convolution, the results are summarized in TABLE II. Interestingly, for the blade speed of 180 mm/s, there was no OH group on the surface. Contrarily, for the speed of 50 mm/s there was a large ratio of 35% of OH group. The high ratio of the polar OH group on the surface may explain the low PCE for the low blade speed. For example, the local electrical dipole of OH group may expel the PCBM away from the interface. The depletion of PCBM would hinder the electron transfer from the active layer to the IGZO electron transport layer. Combining the surface and depth profile of XPS we conclude that the chemical composition of the IGZO film at the surface

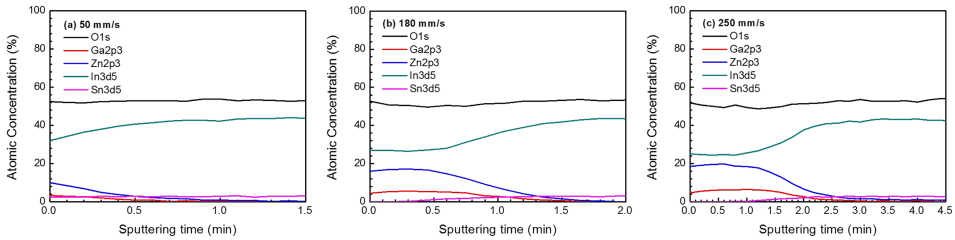

FIG. 11. The IGZO thin films high resolution XPS profile spectra with IGZO blade speed at (a) 50 mm/s (b) 180 mm/s, and (c) 250 mm/s.

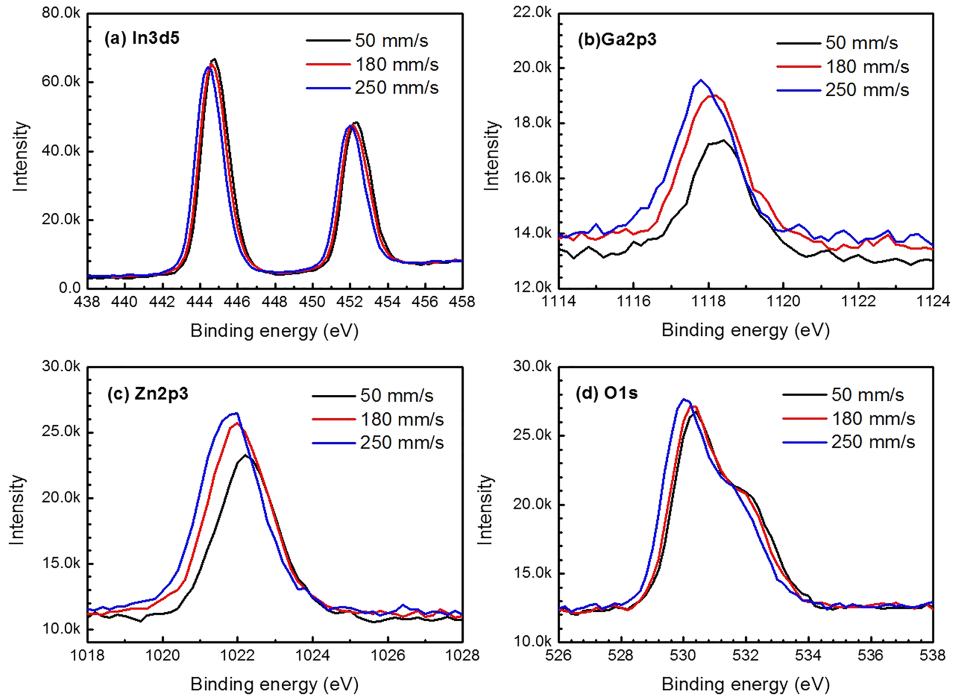

FIG. 12. The IGZO thin films high resolution XPS spectra. (a) In3d5, (b) Ga2p3, (c) Zn2p3, (d) O1s.

and inside can be tuned by the blade speed and the efficiency is correlated with the IGZO surface end group.

One unique feature of the sol-gel reaction in blade coating is the rapid reaction due to the heated substrate as the reaction was initiated at temperature at a moderate 120 °C. In conventional spin coating there is no reaction during coating as it is done in a room temperature. Such rapid reaction appears to give a quite different resulting film. At high blade speed the wet precursor film was first formed, then dried by the substrate heating and hot wind. The drying and sol-gel reaction was therefore away from the precursor reservoir at the blade. On the other hand, at low blade speed the drying took place when the blade was very near as shown in FIG. 13. The sol-gel reaction, therefore occurred in contact with the precursor reservoir, and the reaction products were free to diffuse into and out of the reservoir. Such difference in the drying environment may lead to different reaction chains, and eventually lead to different chemical composition. Such method of chemical tuning of IGZO film may find applications in other areas like thin-film transistors. Besides, the higher wet film thickness at high blade speed implied longer drying time from the heated substrate to the top surface. The period of the drying may also influence the composition.

C. Annealing of active organic layer

In order to optimize the performance, the morphology of the active bulk heterojunction layer was tuned by thermal annealing conditions. The results for annealing at 120 °C and 200 °C of 20 minutes are shown in FIG. 14, and the device characteristics are summarized in TABLE III. The highest PCE

TABLE II. With different sol-gel IGZO blade speed, binding energy of O1s.

B.E. (eV)	50 mm/s	180 mm/s	250 mm/s
530.1	41.65%	51.87%	40.68%
531.4	23.54%	48.13%	56.95%
532.2	34.81%	0.00%	2.38%

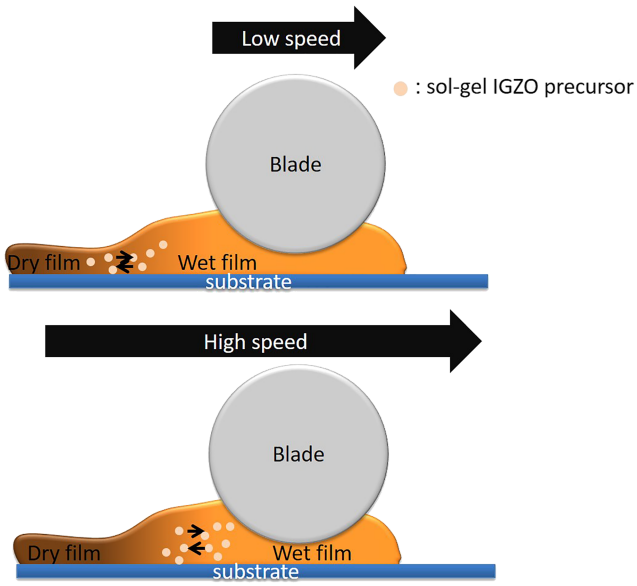

FIG. 13. The diagrams of blade coating at low and high speed.

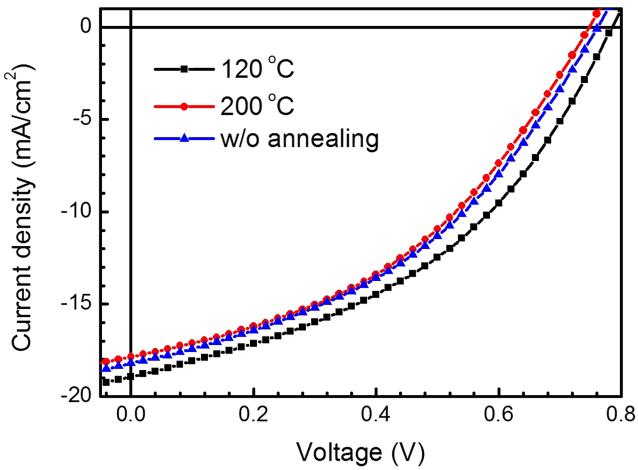

FIG. 14. J-V cure of PBDTTT-C-T/[70]PCBM solar cells annealing on different temperature.

was 6.22% for annealing at 120 °C for 20 minutes, this is slightly higher than the best data in TABLE I, where the annealing time was 10 minutes at 120 °C. The effect of thermal annealing on the surface morphology is shown in the AFM images of FIG. 15. There was no clear difference in the topography. However, for the phase image there were large domains of several hundred nm without annealing whereas the mixing of the polymer and PCBM appeared to be more uniform after annealing. The large single component domain in the blend may reduce the generation of photo-carriers, which took

TABLE III. Photovoltaic parameters for PBDTTT-C-T/[70]PCBM solar cells annealing on different temperature.

Temperature (°C)	PCE (%)	Jsc (mA/cm^2)	Voc (V)	FF
w/o	5.30 ± 0.30	18.50 ± 0.31	0.73 ± 0.02	0.39 ± 0.01
120	6.09 ± 0.13	18.70 ± 0.63	0.78 ± 0.01	0.42 ± 0.01
200	5.00 ± 0.37	16.82 ± 0.67	0.74 ± 0.02	0.40 ± 0.01

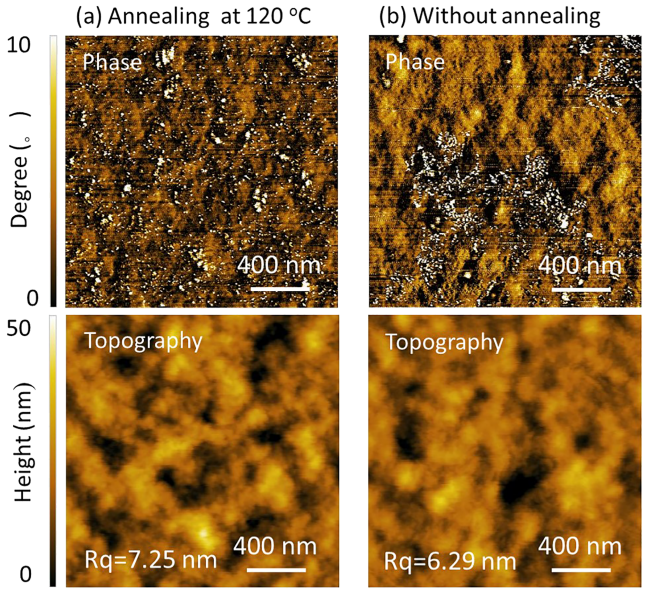

FIG. 15. AFM phase and topography images for active layer (a) annealing at 120°C and (b) without annealing.

TABLE IV. The photovoltaic parameters and thickness of active layer (PBDTTT-C-T/[70]PCBM) with different blend blade speed.

Blend blade speed (mm/s)	PCE (%)	Jsc (mA/cm^2)	Voc (V)	FF
200 (78 nm)	3.96 ± 0.49	12.72 ± 1.06	0.69 ± 0.02	0.42 ± 0.06
300 (112 nm)	5.28 ± 0.25	17.45 ± 0.43	0.76 ± 0.01	0.40 ± 0.01
350 (120 nm)	5.47 ± 0.18	17.99 ± 0.64	0.76 ± 0.01	0.40 ± 0.02
400 (160 nm)	5.35 ± 0.27	16.46 ± 1.09	0.76 ± 0.00	0.43 ± 0.01

place only at the interfaces by excition dissociation. One advantage of our inverted solar cell is that the device survives thermal annealing. In normal structure the PCE dropped dramatically[19] when the PBDTTT-C-T:[70]PCBM blend layer was annealed. The thermal stability of the active layer in the inverted structure may also lead to higher lifetime of the device under sunlight illumination. The dependence of the solar cell performance on the thickness of the organic blend is summarized in Table IV. The optimal thickness is 120 nm achieved by blade coating at 350 mm/s. Such thickness is similar to the one of a normal cell.[19]

D. Comparison with P3HT and ZnO

In order to show that blade coating for IGZO has a general application for organic solar cell, we also study the performance of the device based on the archetypical polymer Poly(3-hexylthiophene-2,5-diyl) (P3HT) and [6,6]-phenyl-C_{61}-butyric acid methyl ester ([60]PCBM). The results are shown in TABLE V. The highest PCE of 3.69% was similar to the normal structure, implying the general application to other organic materials. Finally, we compared our results on IGZO with ZnO for the

TABLE V. Photovoltaic parameters of the P3HT/[60]PCBM and PBDTTT-C-T/[70]PCBM devices with IGZO and ZnO.

Type	Jsc (mA/cm^2)	Voc (V)	FF	PCE (%)
IGZO/P3HT/[60]PCBM	14.20 ± 1.55	0.61 ± 0.00	0.41 ± 0.03	3.56 ± 0.16
IGZO/PBDTTT-C-T/[70]PCBM	16.88 ± 1.37	0.76 ± 0.00	0.43 ± 0.01	5.57 ± 0.35
ZnO/PBDTTT-C-T/[70]PCBM	14.02 ± 0.38	0.78 ± 0.00	0.41 ± 0.01	4.49 ± 0.01

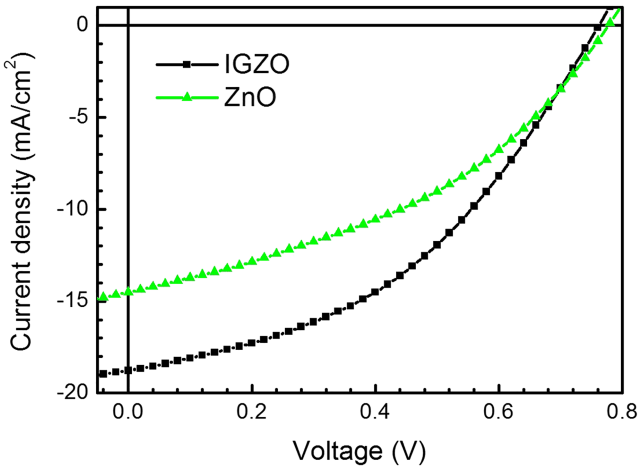

FIG. 16. J-V cures of PBDTTT-C-T/[70]PCBM solar cells with different electron-transport layer.

same furnace annealing at a heating rate of 10 °C/min to a final temperature of 400 °C and maintained for 1 h. The sol-gel precursor of ZnO was made by zinc acetate and dissolved in 2-methoxyethanol at 0.25 M. The results for the two bulk hetero-junction layers are shown in FIG. 16 and TABLE V. For both cases the efficiency for IGZO was higher than ZnO. The superior performance of IGZO may be due to its higher electron mobility, which made the photo-carrier collection easier.

IV. CONCLUSIONS

Uniform IGZO film of several nanometers can be deposited by blade coating with substrate heating using the sol-gel method. The chemical composition and surface functional groups can be controlled by the blade speed. Such IGZO film was used as the electron transport layer for the inverted organic solar cell, where the organic layer was also deposited by blade coating. Using low band-gap polymer, a power conversion efficiency of 6.2% was reached. This fabrication for organic solar cell can be easily scaled up to large area because all the layers are deposited by blade coating except for the top evaporated electrode.

ACKNOWLEDGMENTS

The authors would like to thank Prof. Wen-Bin Jian for helping us to observe IGZO film by atomic force microscope. This work was supported by the National Science Council (NSC) of Taiwan, the Republic of China, under grant NSC 101-2112-M-009-006-MY3.

[1] I. T. Sachs-Quintana, T. Heumüller, W. R. Mateker, D. E. Orozco, R. Cheacharoen, S. Sweetnam, C. J. Brabec, and M. D. McGehee, Advanced Functional Materials **24**, 3978 (2014).
[2] Z. He, C. Zhong, S. Su, M. Xu, H. Wu, and Y. Cao, Nat Photon **6**, 591 (2012).
[3] S. Ho, C. Xiang, R. Liu, N. Chopra, M. Mathai, and F. So, Organic Electronics **15**, 2513 (2014).
[4] T. W. Lee, Y. Chung, O. Kwon, and J. J. Park, Advanced Functional Materials **17**, 390 (2007).
[5] Y.-J. Noh, S.-I. Na, and S.-S. Kim, Solar Energy Materials, and Solar Cells **117**, 139 (2013).
[6] C.-Y. Chen, H.-W. Chang, Y.-F. Chang, B.-J. Chang, Y.-S. Lin, P.-S. Jian, H.-C. Yeh, H.-T. Chien, E.-C. Chen, Y.-C. Chao, H.-F. Meng, H.-W. Zan, H.-W. Lin, S.-F. Horng, Y.-J. Cheng, F.-W. Yen, I.-F. Lin, H.-Y. Yang, K.-J. Huang, and M.-R. Tseng, Journal of Applied Physics **110**, 094501 (2011).
[7] Y.-R. Hong, P.-K. Chen, J.-C. Wang, M.-K. Lee, S.-F. Horng, and H.-F. Meng, Solar Energy Materials and Solar Cells **120**, 197 (2014).
[8] P.-T. Tsai, K.-C. Yu, C.-J. Chang, S.-F. Horng, and H.-F. Meng, Organic Electronics **22**, 166 (2015).
[9] J.-Y. Kwon, D.-J. Lee, and K.-B. Kim, Electron. Mater. Lett. **7**, 1 (2011).
[10] S. J. Heo, D. H. Yoon, T. S. Jung, and H. J. Kim, Journal of Information Display **14**, 79 (2013).
[11] T. Kamiya, K. Nomura, and H. Hosono, Science and Technology of Advanced Materials **11**, 044305 (2010).
[12] K. Shao-Hsuan, H. Ping-Yi, K. Chia-Yu, and L. Ching-Fuh, Photovoltaic Specialists Conference (PVSC) 2013 IEEE 39th (2013) 2723.
[13] H.–C. Liao, C. C. Ho, C.–Y. Chang, M.–H. Jao, S. B. Darling, and W.–F. Su, Materials Today, **16**, 326 (2013).
[14] P.-T. Tsai, H.-F. Meng, Y. Chen, B. Kan, and S.-F. Horng, Organic Electronics **37**, 305 (2016).

[15] P.-T. Tsai, C.-Y. Tsai, C.-M. Wang, Y.-F. Chang, H.-F. Meng, Z.-K. Chen, H.-W. Lin, H.-W. Zan, S.-F. Horng, Y.-C. Lai, and P. Yu, Organic Electronics **15**, 893 (2014).
[16] S.-R. Tseng, H.-F. Meng, K.-C. Lee, and S.-F. Horng, Applied Physics Letters **93**, 153308 (2008).
[17] Y.-H. Chang, S.-R. Tseng, C.-Y. Chen, H.-F. Meng, E.-C. Chen, S.-F. Horng, and C.-S. Hsu, Organic Electronics **10**, 741 (2009).
[18] J.-H. Chang, Y.-H. Chen, H.-W. Lin, Y.-T. Lin, H.-F. Meng, and E.-C. Chen, Organic Electronics **13**, 705 (2012).
[19] Y.-M. Liao, H.-M. Shih, K.-H. Hsu, C.-S. Hsu, Y.-C. Chao, S.-C. Lin, C.-Y. Chen, and H.-F. Meng, Polymer **52**, 3717 (2011).
[20] Y.-F. Chang, Y.-C. Chiu, H.-C. Yeh, H.-W. Chang, C.-Y. Chen, H.-F. Meng, H.-W. Lin, H.-L. Huang, T.-C. Chao, M.-R. Tseng, H.-W. Zan, and S.-F. Horng, Organic Electronics **13**, 2149 (2012).
[21] S.-L. Lim, E.-C. Chen, C.-Y. Chen, K.-H. Ong, Z.-K. Chen, and H.-F. Meng, Solar Energy Materials and Solar Cells **107**, 292 (2012).
[22] E.-C. Chen, P.-T. Tsai, B.-J. Chang, C.-M. Wang, H.-F. Meng, J.-Y. Tsai, Y.-F. Chang, Z.-K. Chen, C.-H. Li, Y.-H. Hsu, C.-Y. Chen, H.-W. Lin, H.-W. Zan, and S.-F. Horng, Japanese Journal of Applied Physics **53**, 062301 (2014).
[23] Y.-F. Chang, Y.-C. Chiu, H.-W. Chang, Y.-S. Wang, Y.-L. Shih, C.-H. Wu, Y.-L. Liu, Y.-S. Lin, H.-F. Meng, Y. Chi, H.-L. Huang, M.-R. Tseng, H.-W. Lin, H.-W. Zan, S.-F. Horng, and J.-Y. Juang, Journal of Applied Physics **114**, 123101 (2013).
[24] P.-T. Tsai, K.-C. Yu, C.-J. Chang, S.-F. Horng, and H.-F. Meng, Organic Electronics **22**, 166 (2015).